Journal of Sound and Vibration (1997) **199**(2), 269–274

AN ADAPTIVE CONTROL SCHEME FOR RECOVERING PERIODIC MOTION OF CHAOTIC SYSTEMS

H. Y. Hu

Institute of Vibration Engineering Research, Nanjing University of Aeronautics and Astronautics, 210016 Nanjing, People's Republic of China

(*Received* 20 *October* 1995, *and in final form* 11 *May* 1996)

The paper presents an adaptive control scheme for recovering the original dynamics of a nonlinear system after a sudden disturbance in a system parameter by controlling the system parameter through linear feedback. The key problem is to choose the control stiffness in the feedback by assigning the poles of the linearized controlled system in an extended state space, which consists of the system state and the system parameter. The paper gives the simulations of recovering the fixed point of the logistic map and the periodic orbit of a harmonically forced Duffing oscillator from the chaos due to a large disturbance in the parameter. The simulations demonstrate well the efficacy and the advantages of the proposed adaptive control scheme.

1. INTRODUCTION

A variety of non-linear mechanical systems in engineering possess several types of steady-state motion attractors, such as periodic orbit, quasi-periodic torus and chaos. The steady-state motion observed in practice depends on one or more system parameters (called control parameters) and the initial state of the system as well. If the control parameter of a system undergoes a large disturbance somehow, the steady-state motion of the system may jump from the present attractor to another attractor. Thus, it is of considerable interest to return the disturbed system to the original attractor through adjusting the system parameters.

Specifically, the steady-state motion of a mechanical system can be described by means of the Poincaré map with a control parameter vector μ

$$\boldsymbol{u}_{k+1} = \boldsymbol{F}(\boldsymbol{u}_k, \mu), \qquad \boldsymbol{u}_k \in R^n, \qquad \mu \in R^m. \tag{1}$$

A simple, but effective control scheme for recovering the original dynamics of a disturbed system is to adjust the control parameter in such a way that its increment is proportional to the difference between the goal state $\boldsymbol{u}_g$ and the current state of the system at discrete time k

$$\mu_{k+1} = \mu_k - \sigma^{\mathrm{T}}(\boldsymbol{u}_k - \boldsymbol{u}_g), \qquad \sigma \in R^{n \times m}, \tag{2}$$

where σ indicates the control stiffness. Huberman and Lumer [1] demonstrated the efficacy of scheme (2) for a one-dimensional map with a control parameter. They found that the recovery time, i.e., the time spent by the recovery process, was proportional to σ^{-1}, $\sigma \in R^1$ in general. Sinha and Ramaswamy [2] applied the scheme to a three-dimensional system with one control parameter and a one-dimensional map with two control parameters.

0022–460X/97/020269 + 06 $25.00/0/sv960630

A key problem in this scheme is to decide on the choice of the control stiffness σ. Sinha [3] pointed out that if the goal state $\boldsymbol{u}_g$ of a one-dimensional map is asymptotically stable and the control stiffness σ is small enough, the scheme will work. To shorten the recovery time, he proposed an algorithm for increasing σ experimentally and applied it to the logistic map successfully. However, the problem remains open for choosing the initial value and for high-dimensional systems.

The primary aim of this paper is to develop a new control scheme to solve the open problem. For brevity, the exposition hereafter is confined to the system having one control parameter, but the extension to the system with more parameters is straightforward.

2. A NEW CONTROL SCHEME BASED ON POLE ASSIGNMENT

The adaptive control scheme suggested in this paper depends not only on the difference between the goal state $\boldsymbol{u}_g$ and the current state $\boldsymbol{\mu}_k$, but also on the difference between the goal parameter μ_g and the current parameter μ_k

$$\mu_{k+1} = \mu_g - \bar{\sigma}^{\mathrm{T}} \begin{bmatrix} \boldsymbol{u}_k - \boldsymbol{u}_g \\ \mu_k - \mu_g \end{bmatrix}, \qquad \bar{\sigma} \in R^{(n+1)\times 1}. \tag{3}$$

To determine the control stiffness $\bar{\sigma}$, equation (1) is linearized in the neighborhood of the goal state $\boldsymbol{u}_g$ that is a fixed point of map (1)

$$\boldsymbol{u}_{k+1} = \boldsymbol{u}_g + \boldsymbol{A}(\boldsymbol{u}_k - \boldsymbol{u}_g) + \boldsymbol{B}(\mu_k - \mu_g), \qquad \boldsymbol{A} \in R^{n\times n}, \qquad \boldsymbol{B} \in R^{n\times 1}. \tag{4}$$

As usual, it is required that the linearized map be controllable with respect to the control parameter. There follows the controllability matrix of rank n

$$\boldsymbol{C} = [\boldsymbol{B} | \boldsymbol{AB} | \cdots | \boldsymbol{A}^{n-1}\boldsymbol{B}] \in R^{n\times n} \tag{5}$$

By combining equation (3) and equation (4), a linearized map of dimension $n+1$ is created,

$$\boldsymbol{v}_{k+1} = \begin{bmatrix} \boldsymbol{u}_{k+1} - \boldsymbol{u}_g \\ \mu_{k+1} - \mu_g \end{bmatrix} = \left(\begin{bmatrix} \boldsymbol{A} & \boldsymbol{B} \\ 0 & 0 \end{bmatrix} - \begin{bmatrix} 0 \\ 1 \end{bmatrix} \bar{\sigma}^{\mathrm{T}} \right) \begin{bmatrix} \boldsymbol{u}_k - \boldsymbol{u}_g \\ \mu_k - \mu_g \end{bmatrix} = (\bar{\boldsymbol{A}} - \bar{\boldsymbol{B}}\bar{\sigma}^{\mathrm{T}})\boldsymbol{v}_k. \tag{6}$$

By choosing an appropriate vector $\bar{\sigma}$ so that all eigenvalues of matrix $\bar{\boldsymbol{A}} - \bar{\boldsymbol{B}}\bar{\sigma}^{\mathrm{T}}$ have modules smaller than unity, the state $\boldsymbol{v}_{k+1}$ will be closer to zero than the state $\boldsymbol{v}_k$ during iteration. Thus, both the system state and the control parameter will approach the goal values. Given the eigenvalues desired, the determination of vector $\bar{\sigma}$ is a problem of pole asssignment for the linearized map (6). The possibility of arbitrary pole assignment depends on the controllability of the linearized map (6), which contains the controllability matrix

$$\bar{\boldsymbol{C}} = [\bar{\boldsymbol{B}} | \bar{\boldsymbol{A}}\bar{\boldsymbol{B}} | \bar{\boldsymbol{A}}^2\bar{\boldsymbol{B}} | \cdots | \bar{\boldsymbol{A}}^n\bar{\boldsymbol{B}}] = \left[\begin{array}{c|c|c|c|c} 0 & \boldsymbol{B} & \boldsymbol{AB} & \cdots & \boldsymbol{A}^{n-1}\boldsymbol{B} \\ 1 & 0 & 0 & & 0 \end{array}\right] = \begin{bmatrix} 0 & \boldsymbol{C} \\ 1 & 0 \end{bmatrix} \in R^{(n+1)\times(n+1)}. \tag{7}$$

Noting that rank $(\boldsymbol{C}) = n$ is equivalent to rank $(\bar{\boldsymbol{C}}) = n+1$, the poles of the controlled system can be assigned arbitrarily by adjusting the control stiffness $\bar{\sigma}$.

From the formula of pole assignment in control theory, the control stiffness to be determined yields

$$\bar{\sigma}^{\mathrm{T}} = [b_{n+1} - a_{n+1}\ b_n - a_n \cdots b_1 - a_1](\bar{\boldsymbol{C}}\bar{\boldsymbol{W}})^{-1}. \tag{8}$$

where

$$\bar{\boldsymbol{W}} = \begin{bmatrix} a_n & a_{n-1} & \cdots & a_1 & 1 \\ a_{n-1} & a_{n-2} & \cdots & 1 & 0 \\ \vdots & \vdots & \vdots & \vdots & \vdots \\ a_1 & 1 & \cdots & 0 & 0 \\ 1 & 0 & \cdots & 0 & 0 \end{bmatrix} \in R^{(n+1)\times(n+1)}, \tag{9}$$

$a_i, \quad i = 1, 2, \ldots, n+1$ are the coefficients of the characteristic polynomial of matrix $\bar{\boldsymbol{A}}$

$$\det(\bar{\boldsymbol{A}} - s\boldsymbol{I}) = \det\begin{bmatrix} \boldsymbol{A} - s\boldsymbol{I} & \boldsymbol{B} \\ 0 & -s \end{bmatrix} = s^n + a_1 s^{n-1} + \cdots + a_n s + 0 \tag{10}$$

and b_i, $i = 1, 2, \ldots, n+1$ are the coefficients of the desired characteristic polynomial of matrix $\bar{\boldsymbol{A}} - \bar{\boldsymbol{B}}\bar{\sigma}^{\mathrm{T}}$.

3. FEATURES OF THE CONTROL SCHEME

In contrast to current control schemes [1–3] the asymptotic stability of the controlled system near the goal state here is independent of that of the original system. The new scheme, therefore, enables one to direct the controlled system to an unstable state of the original system, especially the unstable periodic orbit that is embedded in a chaotic attractor and used as the goal of the OGY control scheme [4–5].

From the comparison of equation (2) with equation (3), it can be seen that the current control schemes are a special form of the new control scheme in the case of

$$\bar{\sigma} = [\sigma_1 \quad \sigma_2 \quad \cdots \quad \sigma_n \quad \sigma_{n+1}]^{\mathrm{T}} = [\sigma^{\mathrm{T}} \quad 1]^{\mathrm{T}} \tag{11}$$

Hence, equation (8) provides a way of choosing the control stiffness σ of the current control schemes under the constraint of $\sigma_{n+1} = 1$.

The above procedure of choosing the control stiffness is based on the linearized map (4), so the control stiffness is effective in the neighborhood of the goal state. If the disturbance in the control parameter is large, the increment of the control parameter determined from equation (3) may exceed a desired tolerance. Thus, it is necessary to impose a saturation/cutoff condition on equation (3) in practice. A natural choice for the cutoff range of the control parameter is the parameter interval from the goal value to the disturbed value.

4. NUMERICAL SIMULATIONS

To make a numerical comparison of the new control scheme with those in references [1–3], a number of control simulations were carried out. For brevity, the term HL will be used to stand for the Huberman-Lumer schemes with constant control stiffness, SV for the Sinha scheme with Variable control stiffness and PA for the new scheme based on Pole Assignment. Furthermore, PA-1 and PA-2 will be used respectively according to whether the constraint $\sigma_{n+1} = 1$ was active or not in the pole assignment procedure of control simulations.

4.1. THE LOGISTIC MAP

The first example chosen is to control the logistic map through an adaptive control parameter μ as follows

$$\begin{cases} u_{k+1} = \mu_k u_k(1 - u_k) \\ \mu_{k+1} = \mu_g - \sigma_1(u_k - u_g) - \sigma_2(\mu_k - \mu_g) \end{cases} \qquad u_k \in [0, 1], \qquad \mu_k, \mu_g \in [0, 4] \tag{12}$$

Figure 1 presents the numerical simulations for returning the map to a stable P-1 fixed point and an unstable P-1 fixed point respectively.

To check the efficacy of the control scheme in recovering a stable $P-1$ fixed point, the parameter was set first at $\mu_k = 1{\cdot}5$, $1 \leqslant k \leqslant 50$ control so that the map had a stable P-1 fixed point $u_g = 0{\cdot}3333$. Then the parameter was altered to $\mu_k = 3{\cdot}9$, $51 \leqslant k \leqslant 100$, where the map behaved chaotically. At $k = 101$, the above four control schemes were initiated to return the map to the original fixed point. The poles of the controlled maps corresponding to PA-1 and PA-2 schemes were placed at $\lambda_{1,2} = (3 - \mu_g)/2$ and $\lambda_{1,2} = 0.0$ respectively. As shown in Figure 1, all schemes could recover the original P-1 fixed point of the map from chaos. However, PA-2 scheme took the shortest recovery time since both poles of the controlled map in this case had the minimal module.

In the second numerical simulation, the parameter was first set at $\mu_k = 3{\cdot}6$, $1 \leqslant k \leqslant 50$ such that the map had an unstable P-1 fixed point $u_g = 0{\cdot}7222$ embedded in a chaotic attractor. Then the parameter was changed to $\mu_k = 3{\cdot}8$, $51 \leqslant k \leqslant 100$. Subsequently, the four control schemes were applied. The poles of the controlled map corresponding to PA-1 and PA-2 schemes were still assigned as $\lambda_{1,2} = (3 - \mu_g)/2$ and $\lambda_{1,2} = 0.0$. As

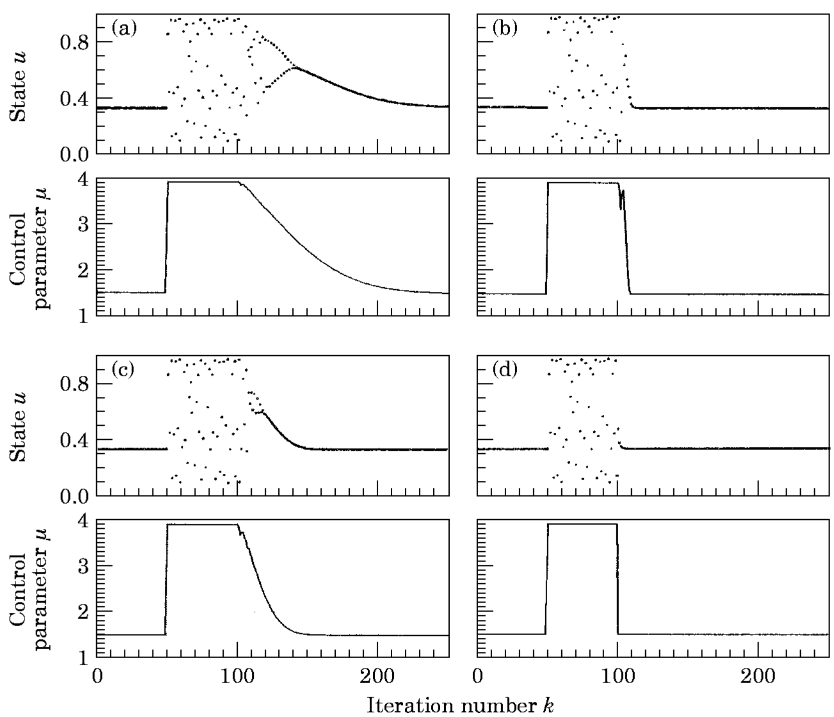

Figure 1. Recovering a stable P-1 fixed point of the logistic map. (a) HL scheme: $\sigma_1 = 0{\cdot}1$, $\sigma_2 = 1{\cdot}0$. (b) SV scheme: $0{\cdot}1 < \sigma_1 < 1{\cdot}6$, $\sigma_2 = -1{\cdot}0$. (c) PA-1 scheme: $\sigma_1 = 0{\cdot}2813$, $\sigma_2 = -1{\cdot}0$. (d) PA-2 scheme: $\sigma_1 = 1{\cdot}125$, $\sigma_2 = 0{\cdot}5$.

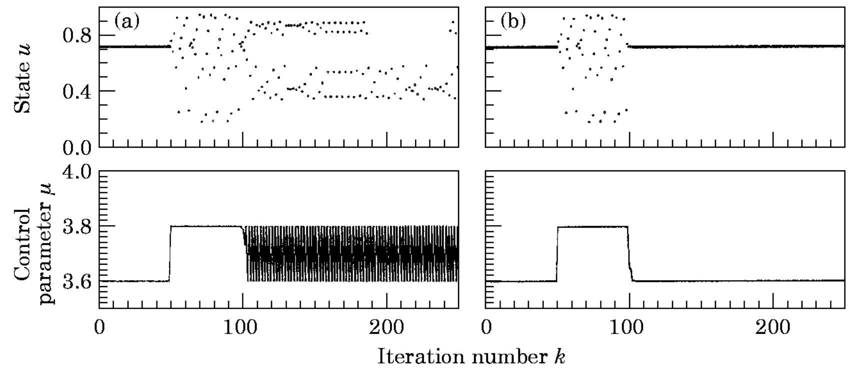

Figure 2. Recovering an unstable P-1 fixed point of the logistic map. (a) SV scheme: $0{\cdot}2 < \sigma_1 < 12{\cdot}8$, $\sigma_2 = -1{\cdot}0$. (b) PA-2 scheme: $\sigma_1 = 12{\cdot}76$, $\sigma_2 = -1{\cdot}60$.

analyzed above, the PA-1 and PA-2 schemes kept working, while the HL and SV schemes failed to direct the disturbed system to the unstable fixed point. For the sake of space, only the control processes of the SV and PA-2 schemes are presented in Figure 2. The comparison of the two schemes shows that the new scheme can direct the system to an unstable fixed point embedded in a chaotic attractor.

4.2. A HARMONICALLY FORCED DUFFING OSCILLATOR

The second example considered was to control a harmonically forced Duffing oscillator by adjusting the excitation amplitude μ;

$$\ddot{x}(t) + 0{\cdot}1\dot{x}(t) + x^3(t) = \mu \cos t. \tag{13}$$

The dynamics of this oscillator with respect to the excitation amplitude μ has been intensively studied. Through the use of stroboscopic sampling at the excitation period $2k\pi$, the forced oscillator can be described by a 2-dimensional Poincaré map with control parameter μ. Thus, all the control schemes mentioned above are directly applicable to the system.

In the simulation, the oscillator was initially at rest and was subject to an excitation of constant amplitude $\mu = 4{\cdot}5$ for the first 100 periods. After a short transient stage, the motion of the oscillator became a stable P-1 orbit. In the next 100 periods, the excitation amplitude was disturbed to $\mu = 7{\cdot}5$ so that the motion of the oscillator was chaotic. Then,

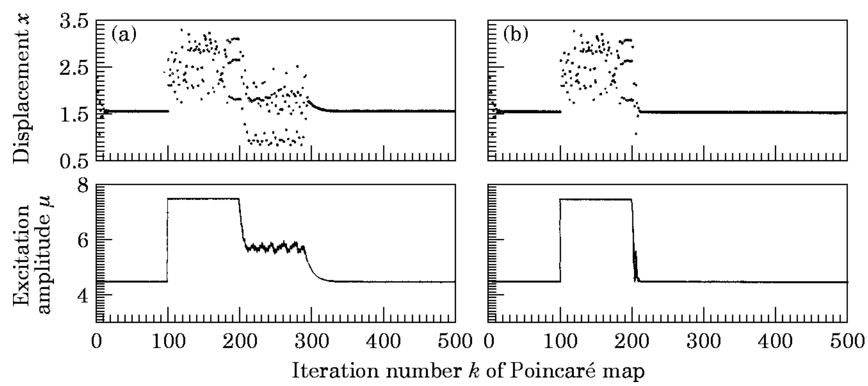

Figure 3. Recovering a stable P-1 orbit of a harmonically forced Duffing oscillator. (a) HL scheme: $\sigma_1 = 0{\cdot}3$, $\sigma_2 = 0{\cdot}0$, $\sigma_3 = -1{\cdot}0$. (b) PA-2 scheme: $\sigma_1 = 1{\cdot}9698$, $\sigma_2 = 0{\cdot}4589$, $\sigma_3 = -1{\cdot}3493$.

the above four control schemes were applied to the oscillator to recover the original stable P-1 orbit. Figure 3 presents the control results of the HL and PA-2 schemes with three poles placed at 0·1, 0·0 and 0·0. The new scheme shows again its advantage over the current schemes in recovery time.

5. CONCLUSIONS

The control scheme suggested here is superior to current schemes proposed by Huberman, Lumer, Sinha, etc. in the following two respects.

(i) The scheme enables one to choose the control stiffness according to desired poles of the controlled system rather than guess the control stiffness or its initial value empirically. As a result, the scheme takes the shortest time to recover the original dynamics of a system.

(ii) The scheme can direct the system to a pre-determined unstable periodic orbit or fixed point, which may be embedded in a chaotic attractor of the system and is used as the goal of the OGY control scheme.

ACKNOWLEDGMENTS

This project is supported in part by The National Natural Science Foundation of China and in part by Trans-Century Training Program Foundation for the Talents by the State Education Commission, China.

REFERENCES

1. B. A. Huberman and E. Lumer 1990 *IEEE Transactions on Circuits and Systems* **37**, 547–550. Dynamics of adaptive systems.
2. S. Sinha and R. Ramaswamy 1990 *Physica D* **43**, 118–128. Adaptive control in non-linear dynamics.
3. S. Sinha 1991 *Physics Letters A* **156**, 475–478. An efficient control algorithm for non-linear systems.
4. E. Ott 1990 *Physical Review Letters* **64**, 1196–1199. Controlling chaos.
5. F. J. Romeiras 1992 *Physica D* **58**, 165–192. Controlling chaotic dynamic systems.